

# Selectivity of Oncolytic Viral Replication Prevents Antiviral Immune Response and Toxicity, but Does Not Improve Antitumoral Immunity

Engin Gürlevik<sup>1</sup>, Norman Woller<sup>1</sup>, Nina Strüver<sup>1</sup>, Peter Schache<sup>1</sup>, Arnold Kloos<sup>1</sup>, Michael P Manns<sup>1</sup>, Lars Zender<sup>1,2</sup>, Florian Kühnel<sup>1</sup> and Stefan Kubicka<sup>1</sup>

<sup>1</sup>Department of Gastroenterology, Hepatology and Endocrinology, Medical School Hannover, Hannover, Germany; <sup>2</sup>Helmholtz Centre for Infection Research, Braunschweig, Germany

Oncolytic infection elicits antitumoral immunity, but the impact of tumor-selective replication on the balance between antiviral and antitumoral immune responses has not yet been investigated. To address this question, we constructed the highly tumor-selective adenovirus Ad-p53T whose replication in target tumor cells is governed by aberrant telomerase activity and transcriptional p53 dysfunction. Telomerase-dependent or nonselective adenoviruses were constructed as isogenic controls. Following infection of mice with the nonselective adenovirus, viral DNA and mRNA levels correlated with strong stimulation of innate immune response genes and severe liver toxicity, whereas telomerase-/p53-specific replication did not trigger innate immunity and prevented liver damage. Compared to telomerase-dependent or unselective viral replication, telomerase-/p53-specific virotherapy significantly decreased antiviral CD8-specific immune responses and antiviral cytotoxicity *in vivo*. Consistent with our hypothesis, telomerase-selective replication led to intermediate results in these experiments. Remarkably, all viruses efficiently lysed tumors and induced a therapeutically effective tumor-directed CD8 cytotoxicity. In immunocompetent mice with extended lung metastases burden, treatment of subcutaneous primary tumors with Ad-p53T significantly prolonged survival by inhibition of lung metastases, whereas unselective viral replication resulted in death by liver failure. In summary, the degree of tumor selectivity of viral replication marginally influences antitumoral immune responses, but is a major determinant of antivector immunity and systemic toxicity.

Received 8 February 2010; accepted 2 July 2010; published online 10 August 2010. doi:10.1038/mt.2010.163

## INTRODUCTION

Upon viral infection, adjusting the magnitude of immune responses is an essential challenge for the host. It has been suggested that the host exploits danger signals of viral infection for

calibration of immune responses that allow successful control of infection but prevent life-threatening inflammation. Viral infection triggers evolutionary conserved innate immune responses leading to tissue inflammation and induction of adaptive immunity. Consequently, it has been shown that antiviral T-cell immune responses strongly depend on recognition of viral DNA and/or single- or double-stranded viral RNA (ssRNA or dsRNA) by host pattern-recognition receptors, demonstrating a close link between innate and adaptive immune responses.<sup>1,2</sup> However, viral infection does not only elicit antiviral immunity but also T-cell immune responses against nonviral antigens by MyD88- and TLR-dependent cross-priming of cellular antigens<sup>3,4</sup> providing an immunotherapeutic approach for tumor-selective, replicating viruses.

Tumor-specific viruses are capable of destroying tumors and even lymph node metastases in immunodeficient animals by intratumoral spreading of infection and tumor-wide oncolysis.<sup>5-7</sup> In immunocompetent animals, the inflammation by the oncolytic virus primarily triggers antiviral immune responses and inhibits virus dissemination,<sup>8,9</sup> but it can also support virotherapy by enhancing antitumoral immune responses and tumor destruction.<sup>10-17</sup> Currently, one of the most important aims in virotherapy is to develop strategies to improve the ratio between antitumoral and antiviral immunity. Recently, some studies investigated innate immune responses and liver toxicity after retargeting of infection of nonreplicating adenoviral vectors with the help of adapter proteins<sup>18</sup> or with fiber modifications.<sup>19,20</sup> Though fiber-pseudotyping led to decreased IL-6 levels and reduced innate immune responses,<sup>19,20</sup> the antiadenoviral adaptive immune response was not significantly affected.<sup>20</sup> Innate immune responses against adenoviral vectors are immediately triggered following cellular entry of viral particles and uptake into the reticuloendothelial system. Splenic proinflammatory macrophages and myeloid dendritic cells have recently been demonstrated to play a crucial role in the induction of anti-Ad innate immune responses involving type I interferon and IL-1 $\alpha$ -dependent signaling pathways.<sup>21,22</sup> With respect to replication-competent oncolytic adenoviruses, accumulation of viral products at later stages of infection may also stimulate innate immune responses. Consequently, targeted

**Correspondence:** Florian Kühnel, Department of Gastroenterology, Hepatology and Endocrinology, Medical School Hannover, Carl Neuberg Str. 1, 30625 Hannover, Germany. E-mail: [kuehnel.florian@mh-hannover.de](mailto:kuehnel.florian@mh-hannover.de) or Stefan Kubicka, Department of Gastroenterology, Hepatology and Endocrinology, Medical School Hannover, Carl Neuberg Str. 1, 30625 Hannover, Germany. E-mail: [Kubicka.stefan@mh-hannover.de](mailto:Kubicka.stefan@mh-hannover.de)

control of viral replication may have a significant impact on adaptive antiviral immune responses and toxicity in virotherapy. Until now, there is no study investigating the correlation of innate and adaptive antiviral immune responses in oncolytic therapy. Furthermore, surprisingly, little is known about the impact of tissue-specific viral replication on the relation between antiviral and tissue-specific immune responses.

Simultaneous targeting of different oncogenic pathways is a suitable way to improve the specificity of oncolytic vectors compared to viruses that are only directed against a single dysfunctional pathway in tumor cells. Because unrestricted replication capability and evading of cell cycle arrest or apoptosis are important hallmarks of cancer,<sup>23</sup> ~90% of human cancers have telomerase activity<sup>24</sup> and the majority of malignant tumors harbor p53 mutations or show abrogation of the p53 pathway through inactivation of other signaling or effector components.<sup>25</sup> Therefore, we exploited these essential tumor characteristics for constructing a highly tumor-selective replicating oncolytic adenovirus (Ad-p53T), which is dependent on telomerase promoter activity as well as transcriptional dysfunction of p53 in the infected target cell. We used the oncolytic virus Ad-p53T and corresponding control viruses to investigate toxicity, innate immune response, and adaptive antiviral and antitumoral immune responses upon tumor-selective or unselective viral replication. Our results demonstrate that viral lysis of tumors elicits a CD8-specific immune response against tumor-antigens, irrespective of the specificity of viral replication. However, restriction of viral replication to tumor cells prevents innate immune responses, toxicity in untargeted tissue, and strongly inhibited adaptive antiviral immune responses during virotherapy.

## RESULTS

### Construction of a highly tumor-selective replicating oncolytic adenovirus that simultaneously targets telomerase and p53 alterations in cancer cells

Replacement of adenoviral early gene promoters by the human telomerase promoter is an established strategy to generate broadly applicable tumor-specifically replicating adenoviruses.<sup>26</sup> However, due to background activity of the telomerase promoter in telomerase-negative, normal cells, adenoviral early protein levels can accumulate to critical threshold levels sufficient for the final onset of replication. Consequently, it has already been shown that adenoviral replication controlled by tumor-specific promoters may result in a loss of selectivity and unwanted side effects, in particular at high multiplicities of infection.<sup>27,28</sup> Loss of p53-transcriptional function is a further fundamental event in carcinogenesis. We therefore considered simultaneous targeting of tumor cell-specific telomerase expression and p53-transcriptional deficiency being a suitable strategy to significantly improve selectivity of oncolytic adenoviruses (the concept is illustrated in **Figure 1a**). In previous works, we showed that stabilization of cellular p53-levels following adenoviral infection can be utilized for p53-deficiency-dependent, tumor-specific gene therapy and oncolytic therapy.<sup>29,30</sup> The system described therein is based on p53-dependent expression of a transcriptional repressor that is directed against synthetic target promoters for the inhibition of viral gene expression in normal cells. To adapt this strategy for

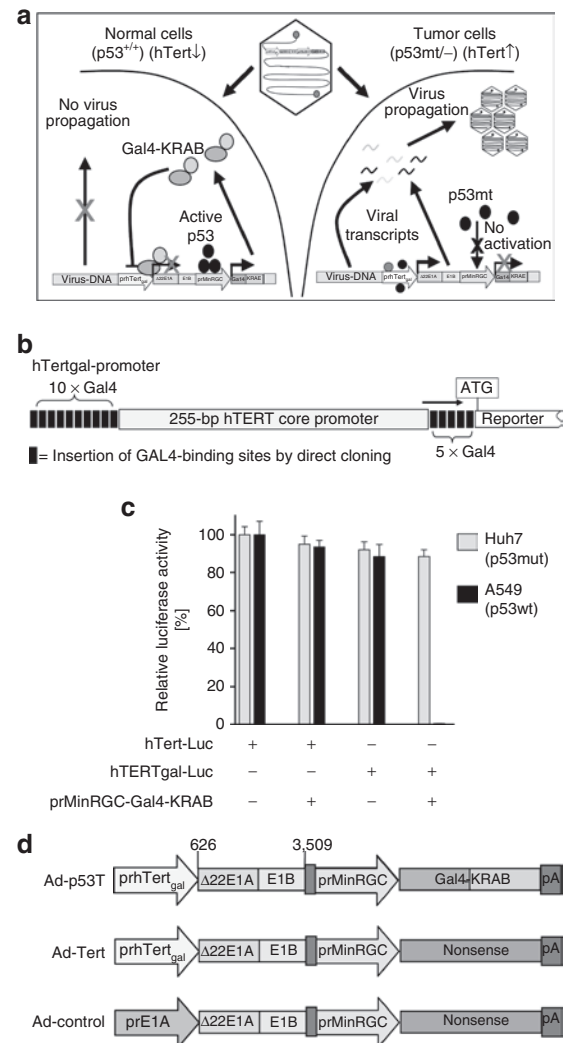


**Figure 1** Generation of highly tumor-specific, oncolytic adenoviruses: hTert/p53-dependent transcriptional targeting of adenoviral replication. **(a)** Illustration showing the concept of hTert/p53-dependent adenoviral replication for highly selective tumor cell targeting. After infection of normal cells, eventual background activity of the E1A controlling hTertgal-promoter is blocked by expression of the transcriptional repressor GAL4-KRAB in response to p53. In tumor cells, p53-dependent GAL4-KRAB response is absent, and full activity of the hTertgal-promoter is released to express E1A to levels required for productive viral replication and cell lysis. **(b)** Scheme that shows the artificial “hTertgal”-variant of the hTert-promoter. The hTert core promoter is flanked by clusters of GAL4-binding sites. **(c)** Susceptibility of the hTertgal-promoter for p53-dependent, GAL4-KRAB-mediated transcriptional repression in p53<sup>+</sup> A549 and p53-mutant Huh7 cells. Luciferase reporter constructs under control of the hTertgal-, or the hTert-promoter, respectively, were co-transfected with prMinRGC-Gal4-KRAB. pSV40-LacZ was co-transfected as internal control. Forty-eight hours after transfection, luciferase signal was determined and normalized by β-galactosidase activity (mean ± SD). The hTertgal-promoter is effectively inhibited by p53-dependent expression of GAL4-KRAB. **(d)** Schematic drawing of generated adenoviruses differing in the quality of tumor-selective replication (Ad-control: nonselective, Ad-Tert: hTert-selective, and Ad-p53T: hTert/p53-selective).

strengthened inhibition of hTert-dependent adenoviral replication, we flanked the hTert core promoter with clusters of binding sites for the transcriptional repressor GAL4-KRAB (**Figure 1b**). The susceptibility of this synthetic promoter (named hTertgal) for

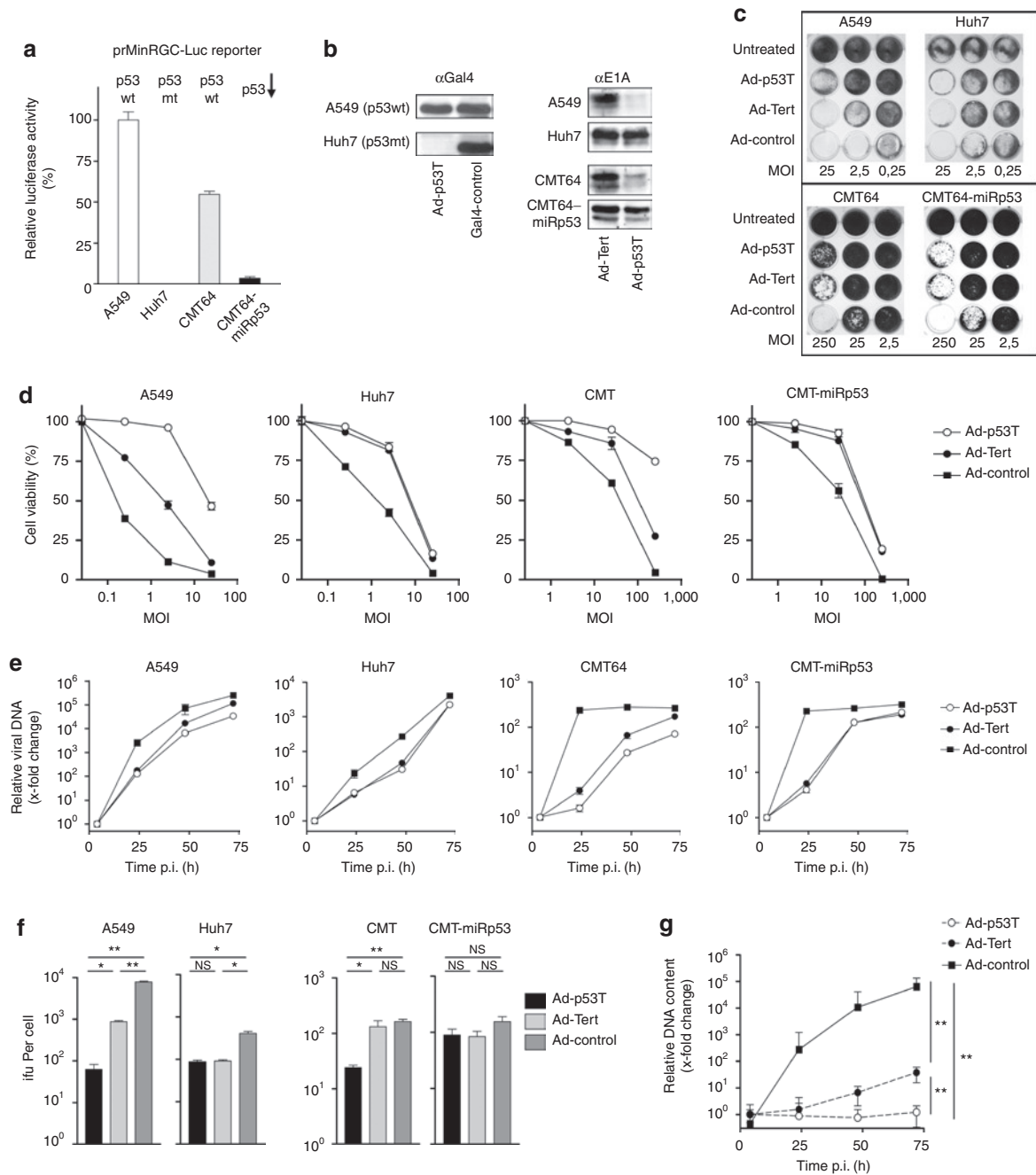


**Figure 2** p53-dependent replication of Ad-p53T *in vitro*. **(a)** Activation of a p53-responsive reporter was investigated in murine CMT64 cells with different p53 status. Cells were co-transfected with a prMinRGC-Luc reporter plasmid and pSV40-LacZ as internal control. Forty-eight hours after transfection, luciferase activity was determined and normalized by  $\beta$ -galactosidase activity (mean  $\pm$  SD). The prMinRGC-promoter is highly active in p53<sup>+</sup> CMT64 cells compared to human A549 cells as positive and p53-mutated Huh7 cells as negative control. Activation is strongly downregulated in p53-knockdown CMT64-miRp53 cells that express a microRNA against p53. **(b)** Gal4-KRAB and E1A levels were visualized by western blot analyses of different cell lines 24 hours postinfection (p.i.) with Ad-p53T and Ad-Tert. Equal loading was confirmed by  $\beta$ -actin blot (data not shown). After infection with Ad-p53T, GAL4-KRAB expression and consequent E1A repression were observable in p53<sup>+</sup> cells but not in p53-dysfunctional cells. **(c,d)** Oncolytic efficacy was determined *in vitro*. Cells were infected with Ad-p53T, Ad-Tert, or Ad-control at different MOIs. All used cells are telomerase-active but differ in their p53 status. Seven to eight days following infection, the extent of cell lysis was visualized by crystal violet staining **(c)** and determined by cell viability assay **(d)**, mean  $\pm$  SD. **(e)** To investigate viral DNA replication, cells were infected with different adenoviruses. MOI of 5 was used for A549 and Huh7 cells, whereas MOI of 50 was used for CMT64 and CMT64-miRp53 reflecting the lower permissivity of these cells for adenoviral transduction. Four, twenty-four, forty-eight, and seventy-two hours postinfection, total DNA was isolated, and the adenoviral DNA content was determined by qPCR. **(f)** Ninety-six hours after infection, viral progeny per infected cell was determined (mean  $\pm$  SD). **(g)** Primary human IMR-90 fibroblasts (telomerase-negative/p53-normal) were infected at MOI 0.1. At the indicated time points, total DNA was isolated and the viral DNA content was determined by qPCR (mean  $\pm$  SD). Together, the results demonstrate that replication of Ad-p53T is regulated in a p53-dependent manner. Due to the complete absence of DNA replication in primary human fibroblasts, Ad-p53T can be regarded as highly tumor-selective, oncolytic adenovirus. \* $P < 0.05$ ; \*\* $P < 0.01$ . ifu, infection forming units; MOI, multiplicity of infection; NS, not significant.

p53-dependent, GAL4-KRAB-mediated transcriptional repression was tested *in vitro* (Figure 1c). Our results demonstrate that GAL4-KRAB, when expressed under control of the p53-dependent prMinRGC-promoter, was sufficient to provide an effective inhibition of hTertgal-dependent reporter expression in p53 wild-type cells, whereas the hTertgal-promoter was fully active in p53-mutated cells. We therefore used this inhibitory loop for construction of the double-targeted oncolytic virus Ad-p53T. The genetic setup of Ad-p53T and Ad-Tert, an isogenic counterpart lacking the p53-dependent repressor function, as well as the unspecific virus Ad-control is shown in Figure 1d.

To allow for investigations on antitumoral and antiviral immune responses in an immunocompetent murine model of oncolytic tumor infection, we selected CMT64 small cell lung cancer cells whose permissivity for productive infection by human adenoviruses is well established.<sup>17,31,32</sup> Using retroviral gene transfer, we generated the p53-knockdown derivative (CMT64-miRp53) by stable expression of a microRNA directed against murine p53. First, activation of the p53-selective promoter prMinRGC, used as p53-sensor element in Ad-p53T, was investigated in these cell lines by luciferase assays (Figure 2a). Human p53<sup>+</sup> A549 and p53-mutant Huh7 cells served as positive and negative control, respectively. We could observe a high expression of the p53-dependent luciferase reporter in CMT64 cells that was almost completely abrogated in CMT64-miRp53 cells, thus confirming successful knockdown of p53. Correct function of the p53-dependent GAL4-KRAB inhibitory loop was further verified by western blots (Figure 2b). In p53<sup>+</sup> cells infected with Ad-p53T, we could detect strong expression of GAL4-KRAB, in contrast to observations in p53-dysfunctional cells. Consistently, p53-dependent GAL4-KRAB expression by Ad-p53T abolished E1A expression in cells with normal p53 activity but not in cells with p53 dysfunction (Figure 2b). The comparison with the telomerase-dependent but p53-independent isogenic virus Ad-Tert confirmed that E1A regulation was solely dependent on the cellular status of p53, but was not explainable by different activation of the hTert-promoter. Oncolysis and cell viability assays showed improved protection of p53-normal cells following infection by Ad-p53T compared to Ad-Tert and the nonselective Ad-control (Figure 2c,d). After application of low multiplicities of infection (MOIs), cytolytic activity of Ad-control was more efficient compared to both telomerase-dependent counterparts reflecting the higher activity of the wt-E1A-promoter used in Ad-control. However, at high viral MOI, thus simulating the situation in oncolytic infections following intratumoral treatments, all viruses were able to kill p53-dysfunctional cells in a comparable manner. Consequently, at the late stage of viral replication, Ad-p53T reached almost similar levels of progeny compared to the control viruses in p53-dysfunctional cells (Figure 2e). Additionally, we could not observe any differences in the formation of infectious progeny per cell after infection with Ad-p53T or Ad-Tert in p53-dysfunctional cells, whereas in p53-active tumor cells, replication of Ad-p53T was significantly inhibited compared to Ad-Tert again confirming the correct function of the p53-dependent inhibitory loop (Figure 2f). To finally assess the benefit of p53-dependent E1A regulation in the nontransformed, telomerase-negative context, primary human fibroblasts were infected and viral DNA replication was determined. In agreement with our previous results,<sup>26</sup> DNA replication of Ad-Tert was strongly inhibited in primary fibroblasts

compared to the nonspecific control virus (Figure 2g). However, the low but detectable DNA replication of Ad-Tert, most likely driven by background activation of the hTert-promoter, could be completely blocked by additional p53-dependent repression of the hTertgal-promoter in Ad-p53T. The observation that Ad-p53T DNA replication can be detected (at least to a low extent) after infection of p53<sup>+</sup> tumor cells, but is completely absent in primary cells, underscores that primary cells better reflect physiologic conditions than transformed cells. In conclusion, we considered Ad-p53T as a highly tumor-selective, oncolytic adenovirus.

### Viral DNA replication and viral mRNA expression in infected livers correlate with induction of innate immune response genes, antiviral immune responses, and liver toxicity

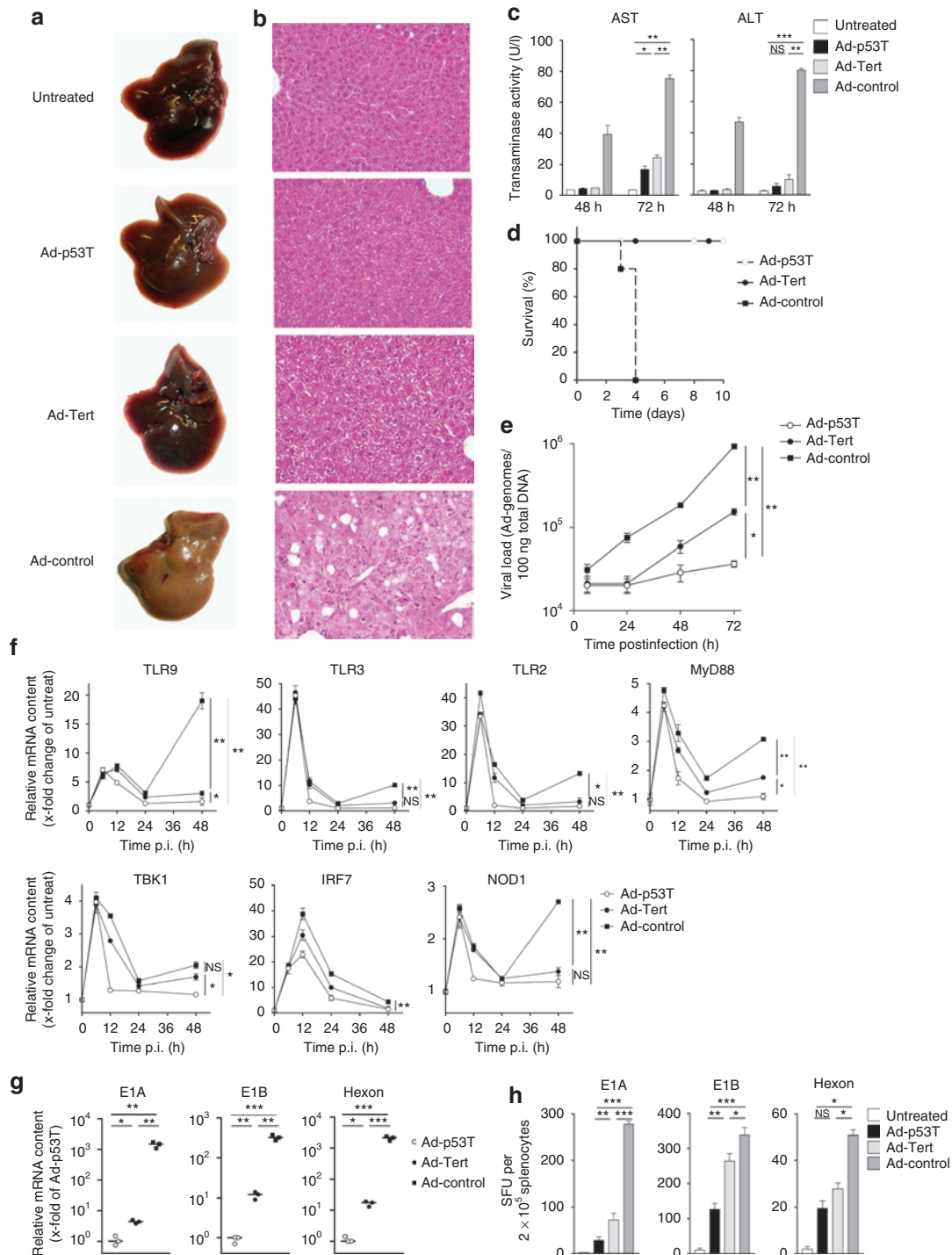
Upon systemic delivery in mice, it is well known that the majority of adenoviruses localize to the liver. We therefore used the liver as nontarget tissue to analyze the effect of selectivity on toxicity and immune responses. Liver tissue destruction was obvious after application of the unselective Ad-control as demonstrated by the macroscopic appearance of explanted livers, corresponding histologies, and dramatically increased levels of transaminases at day 3 following treatment (Figure 3a-c). The extent of liver injury resulted in fatal liver failure within 4 days (Figure 3d). In contrast, livers of Ad-p53T treated animals appeared to be largely unaffected, transaminase activity reached low (alanine transaminase) or modest levels (aspartate transaminase), and all animals survived the treatment. In comparison, mice treated with the less selective virus Ad-Tert survived as well, but showed significantly elevated transaminase levels. To resolve differences on the molecular level, livers were harvested at the indicated time points and investigated for nontumor-targeted viral DNA replication and viral mRNA expression after virus administration (Figure 3e,g). Following Ad-control infection, we observed a strong viral DNA replication. At the late stage of viral replication (48–72 hours), livers infected by Ad-Tert showed a higher increase of viral DNA than following infection by Ad-p53T. Our investigations on viral mRNA expression yielded corresponding results. Next, we analyzed the induction of innate immune response genes in liver tissue following infection. It has been previously reported that systemic delivery of adenoviral vectors provokes an immediate innate immune response with a characteristic peak at 6 hours postinfection<sup>33,34</sup> due to integrin-mediated adenoviral cell entry, detection of viral capsids and lysosomal escape. Because this immediate response can be observed before viral replication is initiated, the level should be independent of the replicative properties of the used vector. Consistently, all three viruses provoked comparable immediate responses of innate immunity genes (Figure 3f). Interestingly, we could observe that expression of innate immune genes was restimulated at late stages of viral infection in treated mice. Because murine liver cells are unable to produce infectious adenoviral progeny, these data suggest that this late innate response is related to the accumulation of viral products and danger signals during the late phase of the replication cycle. Correlating with our results concerning viral DNA replication and mRNA expression, the late induction of innate immune response was most prominent after treatment with Ad-control, but was modest after Ad-Tert

infection and almost absent after Ad-p53T infection as demonstrated for most of the innate immune genes analyzed in this experiment. Consistent with these observations, telomerase-/p53-targeted replication of Ad-p53T elicited significantly lower major histocompatibility complex I-restricted, peptide-specific CD8 immune responses against viral early proteins such as E1A and E1B, or viral structural proteins like hexon, compared to Ad-Tert and the unselective control virus (Figure 3h). However, because unselective viral replication can evoke severe toxic side effects after systemic virus delivery, it cannot be excluded that the strong

induction of innate immune responses in nontarget tissue, e.g., via release of activating cytokines, is able to support antitumoral immune responses during intratumoral viral replication.

**Tightly tumor-restricted viral replication reduces antivector immune responses, but maintains the therapeutically relevant, virotherapy-induced antitumoral immune response**

Next, we investigated the relations of antiviral and antitumoral immune responses after oncolytic therapy in syngeneic mouse



models with subcutaneously grown CMT-miRp53 tumors. We found that administration of low doses of the viruses via the systemic route neither resulted in significant tumor lysis nor in a detectable antitumoral immune response (data not shown). Therefore, mice were treated intratumorally because systemic high-dose treatment caused lethality according to the observations shown in **Figure 3d**. Following intratumoral injection, all viruses caused almost comparable oncolysis as shown by tumor histologies (overview is shown **Figure 4a**, and magnification of the lytic front in **Figure 4b**) and by fluorescence microscopy of tumor sections (**Figure 4c**). Oncolysis was accompanied by massive lymphocyte infiltration into lytic regions suggesting an effective oncolytic inflammation in the tumor. Consistently, high viral load could be detected in the tumor tissue and similar viral DNA replication could be observed in case of all three viruses after treatment (**Figure 4d**). Unexpectedly, a sharp reduction of the viral DNA content in the tumor could be observed between 48 and 72 hours after infection, suggesting ineffective reinfection of tumor tissue after a first round of replication and subsequent systemic release of the viral progeny. However, this was not reflected by the kinetic of the viral load in the livers of the treated animals. The viral DNA content in the liver showed high levels in Ad-control-treated mice, elevated levels in Ad-Tert-treated mice but very low levels in Ad-p53T-infected mice (**Figure 4e**). We could not detect a “second peak” in hepatic viral load that could be related to incoming viral progeny from the infected tumor after 48 hours. In contrast, the kinetic was congruent to a pulsed intravenous infection (as shown in **Figure 3e**), suggesting that the viral liver load almost completely results from tumor leakage during injection and subsequent replication in the liver. With regard to the massive lymphocytic infiltration in the inflamed tumor tissue (**Figure 4b**), these findings rather suggest that infected lytic cells are effectively removed from the tumor tissue by tumor-infiltrating immune cells.

After virus application, we observed similar major histocompatibility complex I-restricted peptide-specific IFN- $\gamma$  release by splenocytes of treated mice upon stimulation with the tumor model antigen GFP in all treatment groups. In contrast, antiviral CD8 immune responses were strongly enhanced in the Ad-control group and significantly elevated in the Ad-Tert group, suggesting a correlation between antiviral immune response and tumor selectivity of the used virus (**Figure 5a**). To analyze whether intratumoral therapy of the primary tumor elicits cytotoxic T-cell responses,

*in vivo* cytotoxic T lymphocyte assays were performed. In agreement with the results above, virotherapy with the highly selective virus Ad-p53T provoked a mild antiviral cytotoxic T-cell response that was enhanced after application of Ad-Tert, and fully developed in the Ad-control group (**Figure 5b**). However, all viruses were capable to induce a significant cytotoxic CD8 immune response against the tumor model antigen. Although antitumoral cytotoxic CD8 response was slightly (but statistically significant) reduced after Ad-p53T and Ad-Tert therapy compared to Ad-control, this difference was therapeutically irrelevant in a mouse model with a low number of lung metastases (**Figure 6a-c**). In this model, local virotherapy of the primary subcutaneous tumor was performed to assess the therapeutic effect of the virotherapy-induced antitumoral cytotoxicity on virally uninfected lung metastases. Intratumoral virotherapy with Ad-p53T or Ad-control inhibited the growth of lung metastases to a comparable extent and resulted in a significant survival benefit compared to untreated mice, thus demonstrating the systemic therapeutic efficacy of the elicited antitumoral cytotoxicity (**Figure 6b,c**).

Finally, to figure out therapeutic differences between highly tumor-selective virotherapy and unselective oncolytic replication, we used a more challenging animal model with increased burden of lung metastases (**Figure 6d**). Because we observed no significant inhibition of metastases after an intratumoral low-dose injection of oncolytic adenoviruses in this model (data not shown), we speculated that repeated application of higher viral doses of the oncolytic virus could be required to obtain a therapeutic benefit for the treatment of a large metastases burden. In this model, untreated animals died at day 18 because of lung metastases, whereas repeated intratumoral application of Ad-control resulted in early death of the animals due to liver failure (**Figure 6e,f**). In contrast, tumor oncolysis with Ad-p53T induced an antitumoral immune response that was capable to delay the outgrowth of disseminated lung metastases (**Figure 6g**), resulting in significantly prolonged survival of the animals (**Figure 6e**). Because Ad-Tert resulted in a similar outcome compared to Ad-p53T at least under these conditions (data not shown), we focused on the demonstration of Ad-p53T as representative for a highly tumor-selective oncolytic adenovirus. In summary, these experiments demonstrate that infection of a primary tumor with an oncolytic adenovirus elicits an antitumoral immune response that is therapeutically effective even in animals with high burden of metastases. Furthermore, our results

**Figure 3** Highly tumor-selective replication after systemic infection *in vivo* prevents from liver damage and reduces antiviral cellular immune responses. **(a,b)** C57Bl/6 mice were treated by i.v. injection of  $2.5 \times 10^9$  ifu of adenoviruses as indicated. Seventy-two hours after infection, livers were explanted and examined either macroscopically **(a)** or by hematoxylin and eosin-stained tissue sections **(b)** for signs of liver damage (example shown as representative of  $n = 3$  mice per group of two independent experiments). **(c)** Forty-eight hours and seventy-two hours after infection, blood samples were drawn, and serum transaminase activity was determined (mean  $\pm$  SD;  $n = 3$  per group). **(d)** Survival was determined following viral treatment as described above ( $n = 5$  per group). **(e)**  $1 \times 10^9$  infectious particles were i.v. injected in C57Bl/6 mice. Total DNA was prepared from liver tissue at different time points after infection. Content of viral DNA genomes per total tissue DNA was determined by qPCR (mean  $\pm$  SD,  $n = 4$  mice in each group). **(f)** Total RNA was isolated from liver tissue at different time points after infection of i.v.-treated C57Bl/6 mice. Relative change of mRNA levels of innate immune response genes were determined by RT-qPCR (mean  $\pm$  SD,  $n = 4$  mice in each group). **(g)** Viral gene expression after i.v. treatment of C57Bl/6 mice was examined of total RNA isolations (mean  $\pm$  SD,  $n = 3$  mice in each group). **(h)** Antiviral cellular immune responses were investigated after systemic treatment of C57Bl/6 (for E1A and E1B) and DBA/2 (for hexon) mice with  $1 \times 10^9$  ifu of adenoviruses as indicated. At day 14 following injection, T cells were isolated from spleen and plated for ELISpot assays. Thirty-six hours after stimulation with major histocompatibility complex class I-restricted peptides, interferon- $\gamma$ -releasing cells, specific for adenoviral E1A, E1B, or hexon, respectively, were counted (mean  $\pm$  SD,  $n = 5$  mice in each group). The results demonstrate that effective attenuation of Ad-p53T in normal tissue prevents from life-threatening hepatotoxicity after systemic vector delivery, and leads to decreased triggering of innate immunity and reduced antiviral cellular immune responses. \* $P < 0.05$ ; \*\* $P < 0.01$ ; \*\*\* $P < 0.0001$ . ALT, alanine transaminase; AST, aspartate transaminase; ifu, infection forming units; NS, not significant; p.i., postinfection.

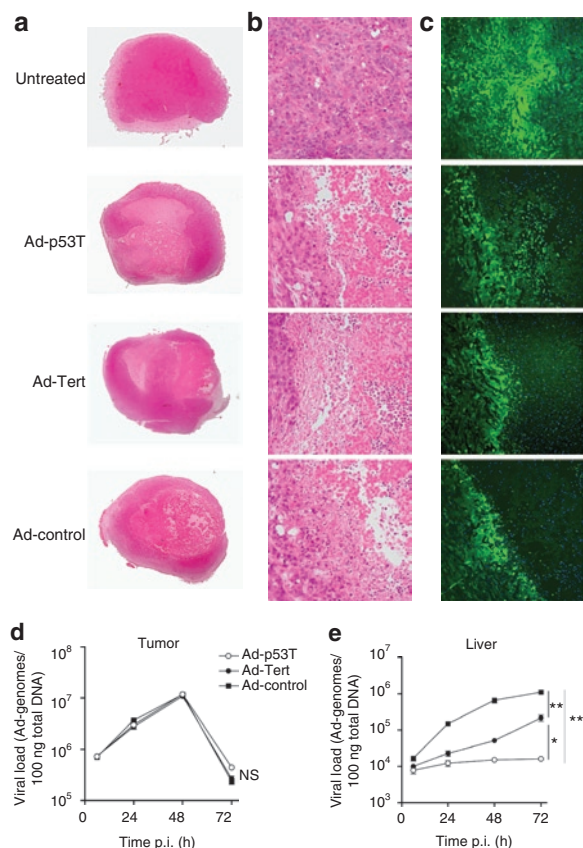


**Figure 4** Tumor treatment with highly selective, oncolytic viruses allows for effective tumor lysis but leads to reduced viral burden in nontarget tissue. Subcutaneously grown CMT64-miRp53 tumors on C57Bl/6 mice were treated twice on subsequent days by intratumoral injection of  $3 \times 10^9$  i.u. of indicated adenoviruses. At day 3 following initial treatment, tumors were isolated and histologically examined by bright field microscopy (complete overview is shown in **a**, magnification of the lytic centers is presented in **b**). **(c)** DAPI-stained tissue slices were investigated by fluorescence microscopy to detect lytic regions (green cells represent living tumor cells because CMT64-miRp53 cells are also transgenic for GFP; blue color: DAPI-stained nuclei). One slide is shown as representative example of  $n = 5$  mice per group). **(d,e)** At 6, 24, 48, and 72 hours following second treatment, tumors and livers were harvested and DNA was prepared. Viral DNA replication in tumor (**d**) and liver (**e**) was quantified by qPCR (mean  $\pm$  SD;  $n = 4$  mice per group per time point). Together, the data show that all used viruses sufficiently lysed tumors following intratumoral application accompanied by a massive lymphocyte infiltration at the locus of oncolytic inflammation. Though comparable levels of viral replication could be observed in the tumors, the virus burden in nontarget tissue (liver) correlated well with tumor selectivity of the investigated viruses. \* $P < 0.05$ ; \*\* $P < 0.01$ . i.u., infection forming units; NS, not significant; p.i., postinfection.

demonstrate that tight restriction of viral replication to the tumor tissue is obligatory to prevent dose-dependent, life-threatening toxicity of virotherapeutic applications.

## DISCUSSION

Tumor infection with oncolytic viruses is an effective cancer therapy in immunocompromised animal models. This virotherapy is capable to overcome resistance against conventional chemotherapy.<sup>35–37</sup> However, partial remissions of tumors have also been reported in clinical phase I/II virotherapy studies.<sup>38</sup> Current

data in immunocompetent animal models<sup>10–17</sup> as well as in clinical trials<sup>39</sup> support the hypothesis that virus-induced antitumoral immune responses significantly contribute to the outcome of the therapy. We recently showed that arming of oncolytic vectors with MIP-1 $\alpha$  and FLT3L resulted in significantly increased antitumoral efficacy due to enhanced antitumoral immune responses, despite a simultaneously enhanced antiviral immune response.<sup>17</sup> However, unselective enhancement of immune responses during cancer therapy appears to be not a promising strategy for clinical application because it would presumably increase the toxicity and side effects of virotherapy in patients.

Although tight restriction of viral replication to malignant cells in virotherapy appears to be a paradigm, until now, no study has examined the role of tumor selectivity of viral replication in the balance between antiviral and antitumoral immune responses. For our investigations, we first constructed a highly tumor-selective replicating virus that would presumably not trigger replication-related innate immune responses outside the targeted tumor tissue. To allow for broad applicability of this oncolytic vector, we targeted viral replication to cellular alterations in telomerase and p53 pathways, which co-incidentally occur in the vast majority of human cancers. After systemic or intratumoral infection, viral replication and viral mRNA expression of the double telomerase-/p53-targeted oncolytic virus were nearly completely abrogated in nontumor liver tissue. This high selectivity resulted in unchanged liver mRNA expression of innate immune response genes at the late stage of viral replication. Additionally, liver toxicity was strongly reduced. In contrast, viral DNA and mRNA levels in the liver due to unselective replication of the control virus (Ad-control) correlated with strong stimulation of the innate immune response and with liver toxicity. However, of most importance was the fact that tumor-restricted replication of Ad-p53T elicited a significantly lower antiviral adaptive CD8 immune response compared to Ad-control and Ad-Tert. Although all viruses, irrespective of the selectivity, replicated at similar levels in the tumor tissue after intratumoral treatment, there was more DNA increase in livers of Ad-control-treated mice and also a slightly higher antitumoral cytotoxic immune response compared to Ad-p53T and Ad-Tert. But our study shows that local viral infection of a tumor elicits a systemic antitumoral CD8 immune response, irrespective of the selectivity of viral replication, indicating that the unspecific inflammation in nontarget tissue does not significantly contribute to the virotherapy-induced antitumoral immune response. However, this apparent advantage of the unselective virus was therapeutically irrelevant in our experiments. Instead of improved antitumoral efficacy, the rapid but unrestricted replication of Ad-control resulted in severe toxicity and was a great hurdle for repeated virotherapy in a mouse model with high tumor burden. In a preclinical mouse model, we recently showed that the antitumoral immune response, which is elicited by viral infection of a primary tumor, is capable to inhibit the outgrowth of virally uninfected lung metastases.<sup>17</sup> In the current study, we used this metastatic tumor model to investigate the impact of the specificity of viral replication on the efficacy and side effects of oncolytic virotherapy. In agreement with the results of toxicity and immune responses after systemic viral infection, we observed striking differences in the outcome of animals with large burden of metastases after injection of the

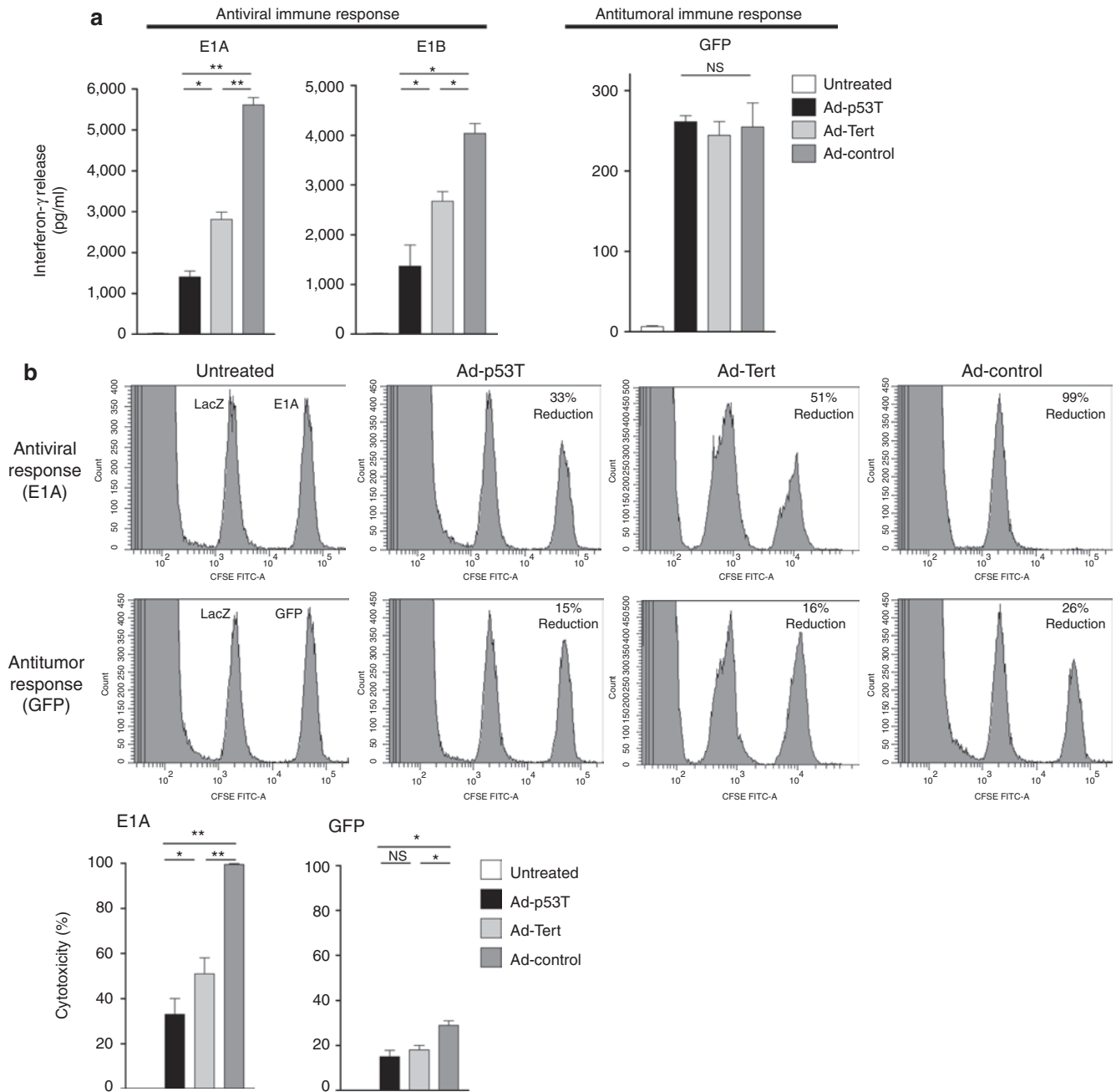


**Figure 5** Oncolytic tumor treatment with highly selective adenoviruses drastically reduces antiviral immune responses, whereas antitumoral response was affected to a minor extent. **(a)** Subcutaneously grown CMT64-miRp53 tumors were treated twice by intratumoral injection with  $3 \times 10^9$  ifu of the indicated adenoviruses. After 14 days, T cells were isolated from spleens to investigate antigen-specific immune responses by enzyme-linked immunosorbent assay. Plated splenocytes were stimulated with major histocompatibility complex (MHC) class I-restricted peptides for E1A or E1B as viral antigens, or GFP as tumor-associated antigen. After 48 hours, antigen-specific interferon- $\gamma$  release was determined in the supernatants of stimulated cells (mean  $\pm$  SD;  $n = 5$  mice in each group). **(b)** An *in vivo* cytotoxic T lymphocyte assay was performed at day 7 following intratumoral treatment of s.c. CMT64-miRp53 tumors. Donor splenocytes were stained with CFSE and different MHC class I-restricted peptides. LacZ was used as control peptide (left peak), and E1A or GFP was used as virus-specific or tumor-specific peptide, respectively (right peak). Splenocytes were then i.v. injected into treated recipient mice. After 18 hours, splenocytes of recipient mice were prepared and analyzed by FACS to determine the peptide-specific cytotoxicity (mean  $\pm$  SD;  $n = 5$  mice in each group). The results demonstrate that stringent tumor selectivity of adenoviral replication strongly reduces antiviral immune responses. In contrast, the results suggest that tumor selectivity has only limited consequences on effective provocation of antitumoral immunity. \* $P < 0.05$ ; \*\* $P < 0.01$ . CFSE, carboxyfluorescein succinimidyl ester; GFP, green fluorescent protein; ifu, infection forming units; NS, not significant.

primary tumor with high doses of the highly selective virus compared to the unselective virus. High-dose virotherapy of the primary tumor with Ad-p53T significantly prolonged the survival by inhibition of the growth of lung metastases, whereas application

of Ad-control resulted in early death of the animals due to liver failure. In contrast to the murine cancer cell line CMT64, that was used in our animal experiments, normal murine tissue is only capable to produce viral DNA, but not infectious particles of



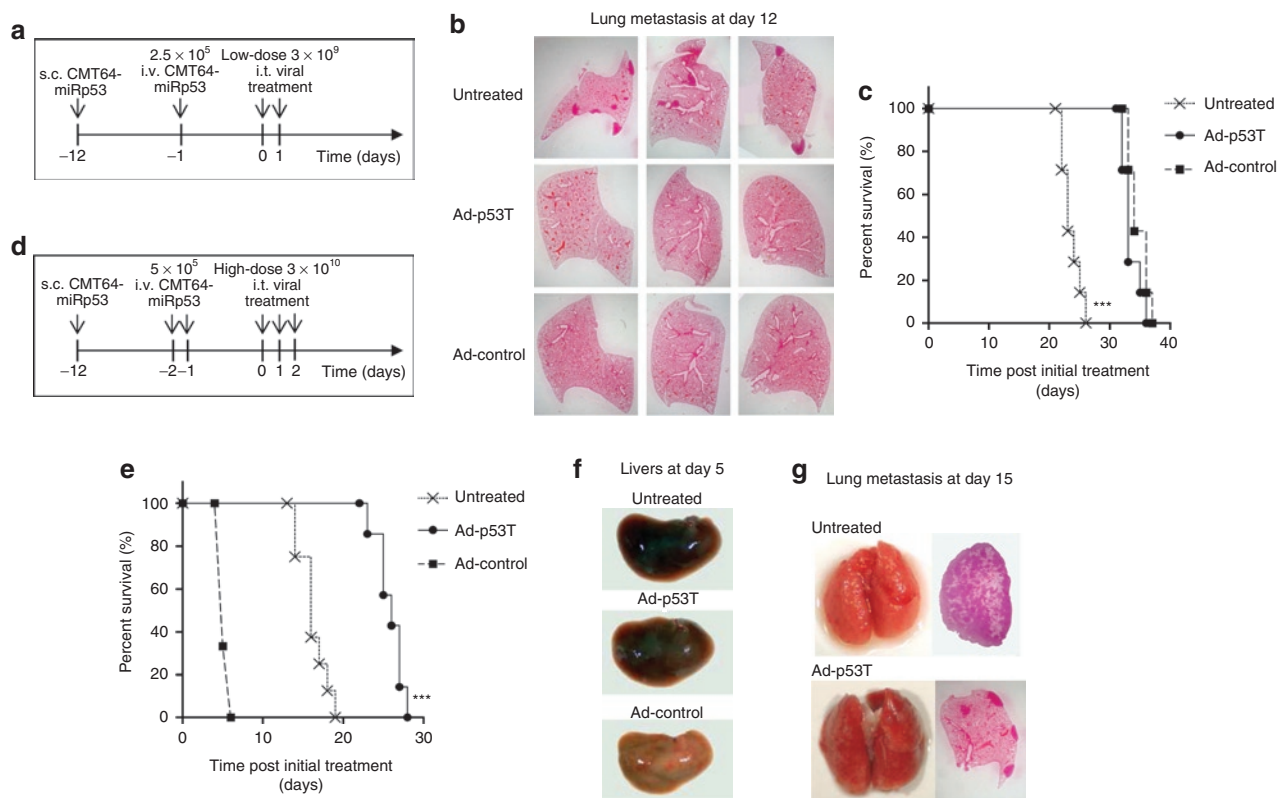


**Figure 6** Highly tumor selectivity of Ad-p53T leads to a therapeutic benefit after high-dose virotherapy in animals with large burden of metastases. Primary s.c. tumors and lung metastases of CMT64-miRp53 cells were established in syngeneic C57Bl/6 mice and subsequently treated according to the therapeutic scheme in **a**. **(b)** At the time of treatment start, primary s.c. tumors were treated twice on two subsequent days by intratumoral injection of  $3 \times 10^9$  i.f.u. Therapeutic efficacy of induced systemic antitumoral immunity was investigated on noninfected lung metastases. For this purpose, mice were harvested at day 12 after initial treatment, lungs were inflated with paraformaldehyde (PFA) solution for fixation, and hematoxylin and eosin (H&E)-stained lung sections were microscopically investigated to determine the lung metastases burden (each image is shown as a representative example of  $n = 3$  mice per group). **(c)** Survival of mice was monitored and determined ( $***P < 0.0001$ , log-rank test;  $n = 7$  mice per group). All animals died due to lung metastases. However, the results show that oncolytic infection of the primary tumor led to significantly prolonged survival. **(d)** Therapeutic scheme of a high-dose tumor treatment model with extended metastases burden: an increased dose of CMT64-miRp53 cells were injected i.v. to induce lung metastases earlier as compared to the previous scheme. Subcutaneously grown tumors (induced at day 12) were threefold i.t. infected with high doses of infectious particles ( $1 \times 10^{10}$  i.f.u.). **(e)** Survival of mice was monitored after treatment according to the scheme in **d** ( $***P < 0.0001$ , log-rank test;  $n = 8$  mice per group). **(f)** Explanted livers at day 5 after initial treatment (one liver as representative example of  $n = 4$  mice per group) were macroscopically investigated for signs of liver injury. **(g)** At day 15, mice were harvested, lungs were inflated with PFA solution for fixation purposes and were examined macroscopically (each image is shown as a representative example of  $n = 3$  mice per group). Extent of lung metastases burden was investigated on H&E-stained lung sections. The results show that viral infection of the primary tumor, irrespective of the degree of selectivity, induces systemic antitumoral immunity that is therapeutically effective against distant, noninfected lung metastases. The results obtained from a model that stringently addresses dose-related toxicity demonstrate that highly tumor-selective adenoviruses can be applied at increased doses to achieve therapeutic efficacy without lethal hepatotoxicity. i.f.u., infection forming units.

human Ad5 (refs. 17,31,32). It seems unlikely that this limitation of our mouse model would have an impact on the antitumoral immune response. Moreover, observable differences in toxicity, innate immune response in the liver, and adaptive antiviral immune responses between Ad-p53T and Ad-control appear to be even understated in our animal model compared to the expected clinical situation in patients.

In summary, our results demonstrate that oncolytic infection of a primary tumor induces a therapeutically effective cytotoxic antitumoral immune response, but the tumor selectivity of viral replication strongly dictates antiviral immune responses and toxicity of virotherapy. Our results therefore justify the multiple efforts that have been undertaken to render viral infection tumor-specific and thus have important implications on the future design of oncolytic viruses.

## MATERIALS AND METHODS

**Cell lines and culturing.** Huh7, A549, 293, and primary human IMR-90 fibroblasts were obtained from ATCC (Rockville, MD). The small cell lung cancer cell line CMT64 was a kind gift from Wilfred Jefferies (Vancouver, British Columbia, Canada). All cells were maintained in DMEM + Glutamax (Life Technologies, Carlsbad, CA) supplemented with 10% heat-inactivated fetal bovine serum (Life Technologies), 100 units/ml penicillin, and 100  $\mu$ g/ml streptomycin (Seromed, Berlin, Germany) at 37°C in 5% CO<sub>2</sub>. CMT64-miRp53 cells were generated by stable transfection of CMT64 with the LMP-construct (Open Biosystems, Huntsville, AL) expressing GFP and a microRNA against p53. For selection of CMT64-miRp53, the medium was additionally supplemented with 1.5 mg/ml puromycin (Calbiochem, Nottingham, UK).

**Genetic construction.** The hTertgal-promoter was generated by insertion of the Gal4-binding sites in the hTert core promoter as previously described,<sup>26</sup> and prMinRGC-Luc and prMinRGC-Gal4-KRAB were

described previously.<sup>29</sup> Shuttle plasmids for the generation of recombinant adenoviruses were constructed on the basis of the plasmid pHM3. The vector pHM3-E1 was constructed previously<sup>40</sup> and includes the  $\Delta$ N22-E1A under control of the wild-type E1A promoter. The vector also contained the E1B region up to the translational stop of E1B-55k (position 3,509). pHM3-hTertgal-E1 was constructed by insertion of the hTertgal-promoter instead of the E1A-wt promoter in pHM3-E1. The p53-dependent expression cassettes for nonsense or Gal4-KRAB expression were inserted downstream of the E1 regions of pHM3-hTertgal-E1 or pHM3-E1 to generate shuttle vectors for subsequent transfer into pAdHM4. Further details concerning cloning procedures or used oligonucleotides can be provided upon request.

**Recombinant adenovirus generation and preparation.** Recombinant adenoviruses were constructed as described.<sup>26</sup> The viral vectors Ad-control, Ad-p53T, and Ad-Tert were generated by ligating the PI-Sce I/I-Ceu I fragments of shuttle pHM3-vectors into pAdHM4. Adenoviral particles were obtained as described previously.<sup>26</sup> Infectious titers of adenoviral preparations were determined by Rapid Titer Kit (Takara/Clontech, Saint-Germain-en-Laye, France) according to the manufacturer protocol.

**Luciferase assay.** Using LipofectAMINE (Life Technologies), cells were co-transfected with 1  $\mu$ g of a firefly luciferase reporter construct and 0.5  $\mu$ g SV40-LacZ for normalization. Total plasmid DNA amount was adjusted to 5  $\mu$ g per 6 cm dish. Twenty-four to forty-eight hours after transfection, cellular extracts were prepared and analyzed for luciferase activity in a Berthold Lumat LB 9501 (Berthold Technologies, Wildbad, Germany) and normalized by  $\beta$ -galactosidase activity measurements.

**Infection of IMR-90 fibroblasts.** To allow efficient infection of IMR-90 fibroblasts, adenoviral vectors were coated with the bifunctional adapter protein CAR<sub>ex</sub>-Tat as described previously.<sup>41</sup> For this purpose, viruses were mixed with purified recombinant CAR<sub>ex</sub>-Tat protein (100 ng/10<sup>4</sup> ifu) and incubated for 15 minutes. 5  $\times$  10<sup>5</sup> IMR-90 fibroblasts were then infected with pretreated viral particles at MOI 0.1.

**Viral DNA quantification.** Using the QIAamp DNA Mini Kit (Qiagen, Hilden, Germany), total DNA was isolated and subjected to quantitative PCR (qPCR MasterMix Plus; Eurogentec, Seraing, Belgium) to determine the viral DNA content. qPCR was performed with 100 ng of DNA using adenoviral hexon-specific primer probes as described before.<sup>42</sup> As internal controls, the 18S genomic control kit (Eurogentec) was applied.

**Reverse transcription qPCR.** Total RNA was isolated using peqGOLD-RNAPure (peQLab, Erlangen, Germany), digested with DNase, and further purified using the RNeasy-Mini-Kit (Qiagen). 100 ng RNA was subjected to reverse transcription using random hexamer primer and TaqMan Reverse Transcription Reagents (Applied Biosystems, Darmstadt, Germany). cDNA was then used for quantification using SYBR Green PCR Master Mix (Applied Biosystems) and 30 cycles with 15 seconds at 95 °C and 60 seconds at 62 °C after a initial step with 10 minutes at 95 °C. The fluorescence signal was acquired at 62 °C. C<sub>t</sub>-values of amplicons were normalized by GAPDH C<sub>t</sub>-values as internal control. Primer sequences for adenovirus and mouse genes were described previously.<sup>40</sup>

**Western blot analysis.** For western blot analysis, cell extracts were prepared by treating the cell layer with a lysis buffer containing 25 mmol/l Tris-phosphate, 2 mmol/l EDTA, 2 mmol/l DTT, 10% glycerol, and 1% Triton X-100. Ten micrograms of protein were separated by SDS-PAGE and transferred onto a PVDF membrane (Immobilon; Millipore, Eschborn, Germany). E1A-proteins were detected using a polyclonal rabbit anti-E1A antibody (Santa Cruz, Heidelberg, Germany). Actin was detected using rabbit antiactin antibody (Santa Cruz). Gal4 was detected using rabbit anti-Gal4 antibody (Santa Cruz). The Western Lightning chemiluminescence reagent Plus (PerkinElmer, Rodgau, Germany) was used for visualization.

**Cytolysis and cell viability assays.** Target cells were seeded in 24-well plates at a density of 4  $\times$  10<sup>4</sup> cells/well and were subsequently infected with adenoviruses at MOIs according to the figure legends. After incubation for 8–10 days, crystal violet staining was used to visualize the destruction of the cell layer. After a gentle rinse with phosphate-buffered saline to remove dead cells, 10% formalin in phosphate-buffered saline was added for fixation (30 minutes). The fixation solution was replaced and cells were then stained for 30 minutes using an aqueous solution of 0.1% crystal violet/10% ethanol. Finally, plates were rinsed with water and air-dried. For cell viability assays, target cells were seeded in 96-well plates at a density of 1  $\times$  10<sup>4</sup> cells/well and were subsequently infected with adenoviruses at MOIs according to the figure legends. After incubation for 7–8 days, cell viability was determined by CellTiter 96 AQ One Solution Cell Proliferation Assay MTS (Promega, Mannheim, Germany) according to the manufacturer's protocol.

**Interferon  $\gamma$ -Elispot.** HTS-PVDF plates (Millipore) were activated with 35% ethanol for 5 minutes, washed three times with phosphate-buffered saline, and incubated with 100  $\mu$ l/well anti-mouse IFN- $\gamma$  antibody (7.5  $\mu$ g/ml, clone: AN-18; eBioscience, San Diego, CA) overnight. After another washing, step plates were blocked with RPMI medium containing 10% fetal calf serum for 2 hours. 2  $\times$  10<sup>5</sup> splenocytes were plated as indicated and incubated with 1  $\mu$ g/1  $\times$  10<sup>6</sup> cells of the corresponding major histocompatibility complex class I-restricted peptides [E1A (SGPSNTPPEI), E1B (VNIRNCCYI), or hexon (KYSPSNVKI)]. After 24 hours, plates were developed by using biotinylated anti-mouse IFN- $\gamma$  (clone: R4-6A2; eBioscience) and streptavidin-HRP (eBioscience). The plates were developed with AEC substrate (Sigma, Hamburg, Germany). Each value was calculated from 8 wells using an ELISpot reader (A-EL-VIS, Hannover, Germany).

**Interferon- $\gamma$  release assay.** 2  $\times$  10<sup>5</sup> splenocytes were plated as indicated in 96-well plates and incubated with 1  $\mu$ g/1  $\times$  10<sup>6</sup> cells/ml of the corresponding peptide. After 48 hours, supernatant were collected and analyzed for IFN- $\gamma$  according to the manufacturer protocol (mouse IFN- $\gamma$  Quantikine ELISA kit; R&D Systems, Minneapolis, MN).

**In vivo cytotoxic T lymphocyte.** Cytotoxic activity and specificity of cytotoxic T lymphocytes were determined by using a carboxyfluorescein succinimidyl ester (CFSE; Molecular Probes, Darmstadt, Germany) based *in vivo* killing assay. Target cells were prepared by using syngeneic splenocytes. After red blood cell lysis, splenocytes were pulsed with according peptide (10  $\mu$ g/10<sup>7</sup> splenocytes/ml) and incubated for 30 minutes at 37 °C. E1A (SGPSNTPPEI) or GFP (DTLVNRIEL) peptide-pulsed splenocytes were then labeled with a final concentration of 2  $\mu$ mol/l CFSE for additional 10 minutes. As control, splenocytes were pulsed with an equivalent concentration of LacZ-peptide (DAPIYTNV) and subsequently stained with 0.2  $\mu$ mol/l CFSE. Both populations were then mixed 1:1 and 2  $\times$  10<sup>7</sup> cells per mouse were injected intravenously. Untreated mice served as control. Specific *in vivo* cytotoxicity was determined by flow cytometric analysis of CFSE<sup>+</sup> splenocytes 18 hours after target cell injection. The ratio *r* between CFSE<sup>hi</sup> and CFSE<sup>lo</sup> cells was calculated to determine effector cell cytotoxicity.

**Animal experiments.** Six- to eight-week C57BL/6 and DBA/2 female mice were obtained from Charles River (Wilmington, MA). All *in vivo* experiments were conducted according to the German legal requirements with approval of Medical School of Hannover animal facility.

Tumors were established by subcutaneous injection of 1  $\times$  10<sup>7</sup> CMT64-miRp53 cells into the flank of mice. Disseminated lung metastases were established by intravenous injection of CMT64-miRp53 cells. Infection of tumors was performed by intratumoral injection according to the figure legends. Intravenous injections of viruses were performed according to the figure legends. DNA and mRNA were isolated as described above. Tissue samples were fixed in paraffin and sections were stained with H&E or DAPI as described previously.<sup>17</sup> To determine serum transaminase

activity, mice were harvested, total blood was drawn from heart and centrifuged for 10 minutes at 6,000g. The serum containing supernatant was used for transaminase assays using the alanine transaminase and aspartate transaminase assay kit (HISS Diagnostics, Freiburg, Germany) according to the manufacturer's protocol.

**Statistics.** For the comparison of two groups, the Student's *t*-test was used to determine statistical significance, and survival curves were analyzed by log-rank test. *P* values < 0.05 were considered as statistically significant.

## ACKNOWLEDGMENTS

This work was supported by Deutsche Forschungsgemeinschaft (DFG) TRR77, DFG KU 1213/3-2, Deutsche Krebshilfe 10–2078-Ku2, and Wilhelm Sander-Stiftung. E.G. constructed the viruses, performed the experiments, interpreted the data, and wrote the manuscript. N.W., N.S., P.S., and A.K. performed the experiments and interpreted the data. L.Z. provided the miRp53 LMP-construct and interpreted the data. F.K. and S.K. designed the study, interpreted the data, and wrote the manuscript.

## REFERENCES

- Huang, X and Yang, Y (2009). Innate immune recognition of viruses and viral vectors. *Hum Gene Ther* **20**: 293–301.
- Saito, T and Gale, M Jr (2007). Principles of intracellular viral recognition. *Curr Opin Immunol* **19**: 17–23.
- Chen, M, Barnfield, C, Näslund, TI, Fleeton, MN and Liljestrom, P (2005). MyD88 expression is required for efficient cross-presentation of viral antigens from infected cells. *J Virol* **79**: 2964–2972.
- Schulz, O, Diebold, SS, Chen, M, Näslund, TI, Nolte, MA, Alexopoulou, L et al. (2005). Toll-like receptor 3 promotes cross-priming to virus-infected cells. *Nature* **433**: 887–892.
- Russell, SJ and Peng, KW (2007). Viruses as anticancer drugs. *Trends Pharmacol Sci* **28**: 326–333.
- Kishimoto, H, Kojima, T, Watanabe, Y, Kagawa, S, Fujiwara, T, Uno, F et al. (2006). *In vivo* imaging of lymph node metastasis with telomerase-specific replication-selective adenovirus. *Nat Med* **12**: 1213–1219.
- Burton, JB, Johnson, M, Sato, M, Koh, SB, Mulholland, DJ, Stout, D et al. (2008). Adenovirus-mediated gene expression imaging to directly detect sentinel lymph node metastasis of prostate cancer. *Nat Med* **14**: 882–888.
- Fulci, G, Breyman, L, Gianni, D, Kurozumi, K, Rhee, SS, Yu, J et al. (2006). Cyclophosphamide enhances glioma virotherapy by inhibiting innate immune responses. *Proc Natl Acad Sci USA* **103**: 12873–12878.
- Altomonte, J, Wu, L, Chen, L, Meseck, M, Ebert, O, Garcia-Sastre, A et al. (2008). Exponential enhancement of oncolytic vesicular stomatitis virus potency by vector-mediated suppression of inflammatory responses *in vivo*. *Mol Ther* **16**: 146–153.
- Bernt, KM, Ni, S, Tieu, AT and Lieber, A (2005). Assessment of a combined, adenovirus-mediated oncolytic and immunostimulatory tumor therapy. *Cancer Res* **65**: 4343–4352.
- Choi, KJ, Kim, JH, Lee, YS, Kim, J, Suh, BS, Kim, H et al. (2006). Concurrent delivery of GM-CSF and B7-1 using an oncolytic adenovirus elicits potent antitumor effect. *Gene Ther* **13**: 1010–1020.
- Lee, YS, Kim, JH, Choi, KJ, Choi, IK, Kim, H, Cho, S et al. (2006). Enhanced antitumor effect of oncolytic adenovirus expressing interleukin-12 and B7-1 in an immunocompetent murine model. *Clin Cancer Res* **12**: 5859–5868.
- Di Paolo, NC, Tuve, S, Ni, S, Hellstrom, KE, Hellstrom, I and Lieber, A (2006). Effect of adenovirus-mediated heat shock protein expression and oncolysis in combination with low-dose cyclophosphamide treatment on antitumor immune responses. *Cancer Res* **66**: 960–969.
- Diaz, RM, Galivo, F, Kottke, T, Wongthida, P, Qiao, J, Thompson, J et al. (2007). Oncolytic immunovirotherapy for melanoma using vesicular stomatitis virus. *Cancer Res* **67**: 2840–2848.
- Thorne, SH, Hwang, TH, O'Gorman, WE, Bartlett, DL, Sei, S, Kanji, F et al. (2007). Rational strain selection and engineering creates a broad-spectrum, systemically effective oncolytic poxvirus, JX-594. *J Clin Invest* **117**: 3350–3358.
- Qiao, J, Kottke, T, Willmon, C, Galivo, F, Wongthida, P, Diaz, RM et al. (2008). Purging metastases in lymphoid organs using a combination of antigen-nonspecific adoptive T cell therapy, oncolytic virotherapy and immunotherapy. *Nat Med* **14**: 37–44.
- Ramakrishna, E, Woller, N, Mundt, B, Knocke, S, Gurlevik, E, Saborowski, M et al. (2009). Antitumoral immune response by recruitment and expansion of dendritic cells in tumors infected with telomerase-dependent oncolytic viruses. *Cancer Res* **69**: 1448–1458.
- Li, HJ, Everts, M, Yamamoto, M, Curiel, DT and Herschman, HR (2009). Combined transductional untargeting/retargeting and transcriptional restriction enhances adenovirus gene targeting and therapy for hepatic colorectal cancer tumors. *Cancer Res* **69**: 554–564.
- Koizumi, N, Yamaguchi, T, Kawabata, K, Sakurai, F, Sasaki, T, Watanabe, Y et al. (2007). Fiber-modified adenovirus vectors decrease liver toxicity through reduced IL-6 production. *J Immunol* **178**: 1767–1773.
- Schoggins, JW, Nociari, M, Philpott, N and Falck-Pedersen, E (2005). Influence of fiber detargeting on adenovirus-mediated innate and adaptive immune activation. *J Virol* **79**: 11627–11637.
- Fejer, G, Drechsel, L, Liese, J, Schleicher, U, Ruzsics, Z, Imelli, N et al. (2008). Key role of splenic myeloid DCs in the IFN- $\alpha$  response to adenoviruses *in vivo*. *PLoS Pathog* **4**: e1000208.
- Di Paolo, NC, Miao, EA, Iwakura, Y, Murali-Krishna, K, Aderem, A, Flavell, RA et al. (2009). Virus binding to a plasma membrane receptor triggers interleukin-1 $\alpha$ -mediated proinflammatory macrophage response *in vivo*. *Immunity* **31**: 110–121.
- Hanahan, D and Weinberg, RA (2000). The hallmarks of cancer. *Cell* **100**: 57–70.
- Harley, CB (2008). Telomerase and cancer therapeutics. *Nat Rev Cancer* **8**: 167–179.
- Brown, CJ, Lain, S, Verma, CS, Fersht, AR and Lane, DP (2009). Awakening guardian angels: drugging the p53 pathway. *Nat Rev Cancer* **9**: 862–873.
- Wirth, T, Zender, L, Schulte, B, Mundt, B, Plentz, R, Rudolph, KL et al. (2003). A telomerase-dependent conditionally replicating adenovirus for selective treatment of cancer. *Cancer Res* **63**: 3181–3188.
- Hurtado Picó, A, Wang, X, Sipo, I, Siemietzki, U, Eberle, J, Poller, W et al. (2005). Viral and nonviral factors causing nonspecific replication of tumor- and tissue-specific promoter-dependent oncolytic adenoviruses. *Mol Ther* **11**: 563–577.
- Bilsland, AE, Merron, A, Vassaux, G and Keith, WN (2007). Modulation of telomerase promoter tumor selectivity in the context of oncolytic adenoviruses. *Cancer Res* **67**: 1299–1307.
- Kühnel, F, Zender, L, Wirth, T, Schulte, B, Trautwein, C, Manns, M et al. (2004). Tumor-specific adenoviral gene therapy: transcriptional repression of gene expression by utilizing p53-signal transduction pathways. *Cancer Gene Ther* **11**: 28–40.
- Kühnel, F, Gurlevik, E, Wirth, TC, Strüver, N, Malek, NP, Müller-Schilling, M et al. (2010). Targeting of p53-transcriptional dysfunction by conditionally replicating adenovirus is not limited by p53-homologues. *Mol Ther* **18**: 936–946.
- Halldén, G, Hill, R, Wang, Y, Anand, A, Liu, TC, Lemoine, NR et al. (2003). Novel immunocompetent murine tumor models for the assessment of replication-competent oncolytic adenovirus efficacy. *Mol Ther* **8**: 412–424.
- Wang, Y, Halldén, G, Hill, R, Anand, A, Liu, TC, Francis, J et al. (2003). E3 gene manipulations affect oncolytic adenovirus activity in immunocompetent tumor models. *Nat Biotechnol* **21**: 1328–1335.
- Hartman, ZC, Kiang, A, Everett, RS, Serra, D, Yang, XY, Clay, TM et al. (2007). Adenovirus infection triggers a rapid, MyD88-regulated transcriptome response critical to acute-phase and adaptive immune responses *in vivo*. *J Virol* **81**: 1796–1812.
- Appledorn, DM, Patial, S, McBride, A, Godbehere, S, Van Rooijen, N, Parameswaran, N et al. (2008). Adenovirus vector-induced innate inflammatory mediators, MAPK signaling, as well as adaptive immune responses are dependent upon both TLR2 and TLR9 *in vivo*. *J Immunol* **181**: 2134–2144.
- Heise, C, Sampson-Johannes, A, Williams, A, McCormick, F, Von Hoff, DD and Kim, DH (1997). ONYX-015, an E1B gene-attenuated adenovirus, causes tumor-specific cytolysis and antitumor efficacy that can be augmented by standard chemotherapeutic agents. *Nat Med* **3**: 639–645.
- Wirth, T, Kühnel, F, Fleischmann-Mundt, B, Woller, N, Djojicubroto, M, Rudolph, KL et al. (2005). Telomerase-dependent virotherapy overcomes resistance of hepatocellular carcinomas against chemotherapy and tumor necrosis factor-related apoptosis-inducing ligand by elimination of Mcl-1. *Cancer Res* **65**: 7393–7402.
- Schache, P, Gurlevik, E, Strüver, N, Woller, N, Malek, N, Zender, L et al. (2009). VSV virotherapy improves chemotherapy by triggering apoptosis due to proteasomal degradation of Mcl-1. *Gene Ther* **16**: 849–861.
- Park, BH, Hwang, T, Liu, TC, Sze, DY, Kim, JS, Kwon, HC et al. (2008). Use of a targeted oncolytic poxvirus, JX-594, in patients with refractory primary or metastatic liver cancer: a phase I trial. *Lancet Oncol* **9**: 533–542.
- Senzer, NN, Kaufman, HL, Amatruda, T, Nemunaitis, M, Reid, T, Daniels, G et al. (2009). Phase II clinical trial of a granulocyte-macrophage colony-stimulating factor-encoding, second-generation oncolytic herpesvirus in patients with unresectable metastatic melanoma. *J Clin Oncol* **27**: 5763–5771.
- Gurlevik, E, Woller, N, Schache, P, Malek, NP, Wirth, TC, Zender, L et al. (2009). p53-dependent antiviral RNA-interference facilitates tumor-selective viral replication. *Nucleic Acids Res* **37**: e84.
- Kühnel, F, Schulte, B, Wirth, T, Woller, N, Schäfers, S, Zender, L et al. (2004). Protein transduction domains fused to virus receptors improve cellular virus uptake and enhance oncolysis by tumor-specific replicating vectors. *J Virol* **78**: 13743–13754.
- Zhang, YA, Nemunaitis, J, Samuel, SK, Chen, P, Shen, Y and Tong, AW (2006). Antitumor activity of an oncolytic adenovirus-delivered oncogene small interfering RNA. *Cancer Res* **66**: 9736–9743.